Korean J. Chem. Eng., **31**(4), 684-691 (2014)
DOI: 10.1007/s11814-013-0269-3

pISSN: 0256-1115
eISSN: 1975-7220

Modeling and simulation of breakthrough curves during purification of two chitosanases from *Metarhizium anisopliae* using ion-exchange with expanded bed adsorption chromatography

Sergio Carvalho de Santana*,,***, Raimundo Cosme da Silva Filho**, Jorge dos Santos Cavalcanti**, Jackson Araujo de Oliveira**, Gorete Ribeiro de Macedo**, Francine Ferreira Padilha*,***, and Everaldo Silvino dos Santos**,†**

*Northeast Biotechnology Network (RENORBIO), Tiradentes University (UNIT), Aracaju/SE, Brazil
**Biochemical Engineering Laboratory, Department of Chemical Engineering,
Federal University of Rio Grande do Norte (UFRN), Natal/RN, 59072-970, Brazil
***Technology and Research Institute (ITP), Biomaterial Laboratory (LBMAT), Av. Murilo Dantas 300,
Farolândia, Aracaju/SE, 49032-490, Brazil
(*Received 24 June 2013 • accepted 8 December 2013*)

Abstract−A mathematical model was developed to predict breakthrough curves during purification of the two chitosanases from *Metarhizium anisopliae* by expanded bed adsorption, taking into account the axial dispersion of liquid and using Streamline DEAE and SP XL adsorbents, anion and cation exchange resins, respectively. All the experiments were performed without clarification (with cells) aiming at the reduction of unit operations in future projects of separation processes, thereby reducing capital and operating costs. Chitosanases are enzymes that hydrolyze the carbohydrate chitosan, resulting in oligosaccharides that have many remarkable biological activities, such as anti-cancer, anti-HIV and antioxidant activities. The two adsorbents had similar performance in relation to hydrodynamics and mass transfer. The results of the parametric sensitivity analysis agree with the literature, and the model was validated with an average high degree of fit (94.68%) between simulated and experimental data obtained in this work.

Keywords: Modeling, Expanded Bed Adsorption, Purification, Chitosanase, *Metarhizium anisopliae*

INTRODUCTION

The combination of modeling with experiments and chromatography theory provides a set of elements that ensure the rational development of a process. This allows a significant reduction in the number of experiments necessary because the model parameters can be estimated from a limited number of experiments. The simulations with the model complement this development and may support the design and development process, identification of critical process parameters and critical sources of variability, studies on management of process variability, analysis of aberrations and process validation [1].

Expanded bed adsorption chromatography allows for the direct purification of bioproducts from unclarified feedstocks, avoiding biodegradation or proteolysis of the target products [2]. Ion-exchange is a traditional and powerful chromatographic technique, based on the net charge between the ligand at the resin stationary phase and the biomolecule surface to effect the separation, and this technique is widely used in the downstream processing of proteins [3-5].

Many single enzymes have been purified with expanded bed adsorption, such as alkaline lipase [6], penicillin G acylase [7], alcohol dehydrogenase [8] and xylanase [9]. Multiple enzymes also have been purified, and *Aspergillus* CJ22-326 with two enzymes [10] is an example; however, it does not use expanded bed adsorption as in the present study with the purification of two chitosanases from *Metarhizium anisopliae*, which is an entomopathogenic filamentous fungus used in biological control [11]. *Metarhizium anisopliae* belongs to the order *Moniliales* and family *Moniliaceae* [12].

Chitosanases (EC 3.2.1.132) represent a class of hydrolytic enzymes that catalyze the β-(1→4) glycosidic bond hydrolysis of chitosan, a linear polysaccharide composed of β-(1→4)-linked D-glucosamine residues, to produce glucosamine oligosaccharides, called chitooligosaccharides [13,14].

Chitooligosaccharides have many remarkable biological activities. They are non-toxic and have anti-cancer, anti-metastatic [15], anti-HIV [16], hepatoprotective [17], antioxidant [18], hypocholesterolemic, antimicrobial, immunostimulating and anti-inflammatory activities [14]. They also are traditionally processed by chemical reaction, which has faced many problems, such as difficulty in controlling the hydrolysis reaction, production of a large amount of short-chain and inexpensive oligosaccharides, a high cost of separation, and possible environmental pollution from the acidic hydrolysis. Hence, obtaining these chitooligosaccharides by hydrolysis with chitosanases has become an important alternative in recent years, with the advantage in terms of environmental compatibility, low cost and reproducibility [14,16].

Highlighting some of the models proposed over time that have contributed for the development of expanded bed adsorption technology of protein adsorption in expanded bed adsorption, there is a starting model developed by Fan et al. [19]. They developed a mathe-

†To whom correspondence should be addressed.
E-mail: everaldo@eq.ufrn.br

matical model applied to fluidized beds for solid-liquid systems, with reference to the adsorption of phenol on granular activated carbon, taking into account hydrodynamic flows, mass transfer and also intraparticle diffusion. Veeraraghavan et al. [20] presented a model of adsorption on solid-liquid fluidized bed, also using granular activated carbon for adsorption of phenol from an aqueous feedstock, which took into account the axial dispersion and the effects of mass transfer, but this model has shown some deviations between the simulations and the experimental data. Thelen and Ramirez [21] developed a model to describe the diffusive characteristics of solid-liquid fluidized systems, predicting the evolution of the height of a bed under conditions of increase and decrease of the fluidization speed. Shortly after, Wright and Glasser [22] developed a model with a better fit between experimental and simulated data. This mathematical model predicts the breakthrough curve of adsorption of a protein in fluidized/expanded beds, taking into account the effects of mass transfer of both the intraparticle diffusion as in the film, besides the effects of adsorption and hydrodynamics, including the axial dispersion of liquid and particle adsorbent [22]. Several other mathematical models have contributed for the development of expanded bed adsorption technology, but generally keeping the core group previously established for the modeling of breakthrough curves [4,23,24].

In this context, our main objective was to develop a mathematical model to predict breakthrough curves to the purification, by expanded bed adsorption, of two chitosanases from *Metarhizium anisopliae.* The model takes into account the axial dispersion of liquid, and used ion-exchange adsorbents, i.e., Streamline DEAE and SP XL adsorbents, which are anion and cation exchange resins, respectively. In addition, the experiments were performed without clarification (with cells), aiming at the reduction of unit operations in the separation processes.

EXPERIMENTAL

1. Chemicals

Streamline DEAE and SP XL adsorbents, anion and cation exchange resins, respectively (GE healthcare, Uppsala, Sweden), both especially designed for expanded bed adsorption. Commercial chitosan (85% deacetylated - POLYMAR/CE- Brazil) was used for the culture medium and as a substrate for enzyme activity. The measurement of chitosanase activity used D-Glucosamine (Sigma, MO/USA) as a standard for the measurement of chitosanase activity. All other chemicals were of reagent grade.

2. Microorganism

EMBRAPA Genetic Resources and Biotechnology (Brasilia/DF-Brazil) kindly provided the fungus *Metarhizium anisopliae* strain (CG374) used in this study.

3. Chitosanase Production Using *Metarhizium anisopliae*

The inoculum of *Metarhizium anisopliae* for enzymes production consisted of spores collected from a potato dextrose agar (PDA) plate after five days of growth. To standardize the inoculum conditions, the spores were suspended in sterile water and reached an optic density (O.D.) of 3.0 as recorded by a spectrophotometer (Thermospectronic Genesys 10 UV-Vis).

For the production of enzyme, we used the pH 6.5 medium (in $g \cdot L^{-1}$) as follows: chitosan 2.0, K_2HPO_4 1.0, $MgSO_4$ 0.5, KCl 5.0, yeast extract 3.0, peptone 5.0, $NaNO_3$ 2.0, and $FeSO_4$ 0.01. Erlenmeyer flasks (250 mL) containing 180 mL of culture medium and 20 mL of inoculums were incubated for 18 hours in a rotating incubator at 147 rpm and at 27 °C. After cultivation the broth was then used directly in the experiments of expanded bed adsorption (without clarification). All measurements were done in triplicate.

4. Protein Determination and Enzyme Activity

The determination of total protein was performed in accordance to the Sedmak and Grossberg modified method [9], measuring absorbance at 595 nm/465 nm with bovine serum albumin (BSA from Sigma Aldrich-Ohio-USA) as the standard protein. Enzyme activity was evaluated determining the amount of reducing sugars generated by hydrolysis of 0.5 mL of chitosan solution (pH 6.5) with 0.5 mL of fermented broth. The reaction was performed for 30 minutes at 55 °C and terminated with 2.5 mL of dinitrosalicylic acid (DNS). The mixture was boiled for 10 minutes followed by cooling in an ice bath. The reduced sugars were quantified recording the absorbance at 600 nm using a standard curve with D-glucosamine. One unit (U) of chitosanase is defined as the amount of enzyme that is capable of releasing 1.0 μmol of reducing sugar equivalent to glucosamine per minute under the assay conditions.

5. Purification with Expanded Bed Adsorption

A chromatography system of expanded bed adsorption (Fig. 1) was used for the experiments of purification of the feedstock with the Streamline DEAE and Streamline SP XL adsorbents.

The glass column (2.6 cm×30.0 cm) used in this work was fitted with an adjustable piston to minimize the headspace over the fluidized bed. A perforated distributor, placed at the bottom of the column, consisted of a stainless steel perforated plate with five holes of 1.0 mm in diameter providing 0.8% of open area. A 60-mesh screen was put below the perforated plate distributor. The column

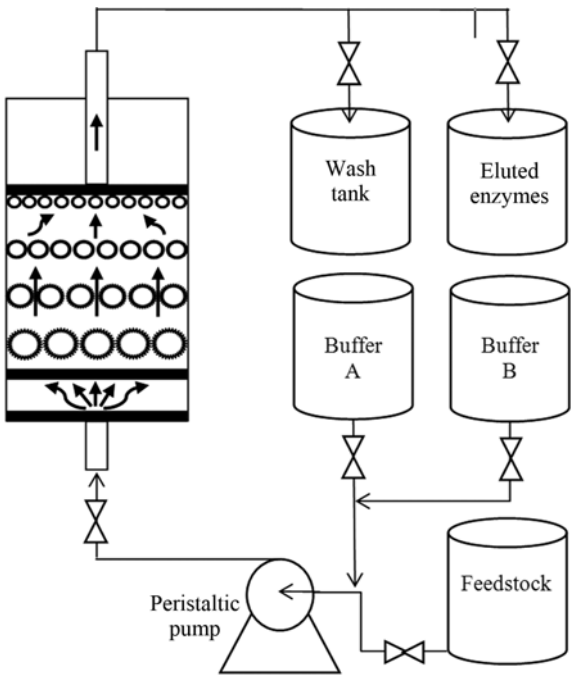

Fig. 1. Expanded bed adsorption system used for all the experiments of purification of the two chitosanases without clarification, showing column (with the expanded and classified adsorbent), pump, valves and tanks.

Table 1. Global parameters estimated for five different simulations with the mathematical model of the purification of two chitosanases from *Metarhizium anisopliae* with expanded bed adsorption[a]

Parameter	Simul. 1	Simul. 2	Simul. 3	Simul. 4	Simul. 5
u ($m \cdot s^{-1}$)	4.17×10^{-4}	7.22×10^{-4}	1.11×10^{-4}	5.69×10^{-4}	2.64×10^{-4}
Ho (m)	7.0×10^{-2}	7.0×10^{-2}	7.0×10^{-2}	7.0×10^{-2}	7.0×10^{-2}
H (m)	18.0×10^{-2}	22.0×10^{-2}	15.0×10^{-2}	20.0×10^{-2}	17.0×10^{-2}
H/Ho	2.57	3.14	2.14	2.86	2.43
Co ($kg \cdot m^{-3}$)	8.33×10^{-3}	8.33×10^{-3}	8.33×10^{-3}	8.33×10^{-3}	8.33×10^{-3}
ε_o	0.4	0.4	0.4	0.4	0.4
ε_p	0.85	0.85	0.85	0.85	0.85
ρ_p ($kg \cdot m^{-3}$)	1200	1200	1200	1200	1200
R (m)	100×10^{-6}	100×10^{-6}	100×10^{-6}	100×10^{-6}	100×10^{-6}
k_f ($m \cdot s^{-1}$)	0.6×10^{-8}	3.2×10^{-9}	3.1×10^{-9}	2.6×10^{-9}	0.6×10^{-8}
D_e ($m^2 \cdot s^{-1}$)	3.5×10^{-11}	3.5×10^{-11}	3.5×10^{-11}	3.5×10^{-11}	3.5×10^{-11}
D_{ax} ($m \cdot s^{-1}$)	1.5×10^{-7}	5.05×10^{-6}	1.5×10^{-7}	5.05×10^{-6}	1.5×10^{-7}
D_s ($m \cdot s^{-1}$)	3.2×10^{-8}	8.8×10^{-8}	0.3×10^{-8}	5.7×10^{-8}	1.4×10^{-8}
q_{max} ($kg \cdot m^{-3}$)	56	56	56	75	75
k_d ($kg \cdot m^{-3}$)	0.38	0.38	0.38	0.06	0.06

[a]Simulations 1, 2 and 3 refer to Streamline DEAE adsorbent; Simulations 4 and 5 refer to adsorbent Streamline SP XL

was coupled to a peristaltic pump (model Perimax 12, Spetec) which was used for pumping both buffers A and B, and the feedstock, as shown in the Fig. 1.

Runs were performed without clarification. The column with 7.0 cm settled-bed height of resins was equilibrated with a 50 mM phosphate pH 6.5 buffer (buffer A). The broth was then loaded (flow-through step) onto this column at the superficial velocity required according to Table 1. The next step of this purification was washing, with superficial velocity of 80 $cm \cdot h^{-1}$, following the elution with a 50 mM phosphate pH 6.5 buffer containing 1 M NaCl (buffer B) at the superficial velocity of 80 $cm \cdot h^{-1}$, keeping the composition of this mobile-phase constant, i.e., performing the elution under isocratic conditions. Several fractions were collected for enzyme quantification and all purification steps (flow-through, washing and elution) were performed at ambient temperature (25 °C), and maintaining the expanded bed with upward flow for all the steps.

MODEL DEVELOPMENT

The modeling of a breakthrough curve is governed by a set of partial differential equations, each one contributing with a certain aspect that is taken into account in the model to make it as accurate as possible in relation to the experimental data [25,26]. We highlight that we have modeled the breakthrough curves considering enzyme activity as a monocomponent protein since both profiles were quite similar.

The adsorption equilibrium was represented with the Langmuir isotherm equation, whereas the protein concentration in the pore of the adsorbent is in local equilibrium with its concentration adsorbed on the inner surface of the pore wall:

$$q^* = \frac{q_m C^*}{k_d + C^*} \tag{1}$$

where q^* is the protein concentration adsorbed on the resin, C^* is the protein concentration in the liquid at equilibrium, and the parameters q_m and k_d are, respectively, the maximum concentration that the solid phase can adsorb, and the constant that measures the degree of affinity between the adsorbent and adsorbate [24].

A basic assumption for the model is that the rate of protein adsorption to the adsorbent is controlled by pore diffusion and external liquid-film mass transfer resistances [27]. Assuming also that the hydrodynamic behavior of solid and liquid phases can be described by an axial dispersion model [28], we used the following equation and the initial and boundary conditions for the axial dispersion of liquid phase [23]:

$$\frac{\partial C}{\partial t} = D_{ax}\frac{\partial^2 C}{\partial z^2} - \frac{u}{\varepsilon}\frac{\partial C}{\partial z} - \frac{3k_f(1-\varepsilon)(C-C_f)}{\varepsilon R} \tag{2}$$

I.C.: at t=0; C(z, 0)=0 for $0 \le z \le H$

B.C.1: at z=0; $C = C_0 + \frac{\varepsilon D_{ax}}{u}\frac{\partial C}{\partial z}$ for t>0

B.C.2: at z=H; $\frac{\partial C}{\partial z} = 0$ for t>0

The equation used for the dispersion of the solid phase, in turn, can be described by [22]:

$$(1-\varepsilon)\frac{\partial \bar{q}}{\partial t} = D_s\frac{\partial^2 \bar{q}}{\partial z^2} + \frac{3k_f(1-\varepsilon)(C-C_f)}{R} \tag{3}$$

I.C.: at t=0; $\bar{q}(z, 0)=0$ for $0 \le z \le H$

B.C.1: at z=0; $\frac{\partial \bar{q}}{\partial z}=0$ for t>0

B.C.2: at z=H; $\frac{\partial \bar{q}}{\partial z}=0$ for t>0

Closing the basic set of equations necessary for modeling of an expanded bed adsorption, the intraparticle continuity equation used can be represented by [27]:

$$\varepsilon_p\frac{\partial c_i}{\partial t} + \frac{\partial q_i}{\partial t} = \varepsilon_p D_e\left(\frac{\partial^2 c_i}{\partial r^2} + \frac{2}{r}\frac{\partial c_i}{\partial r}\right) \tag{4}$$

I.C.: at t=0; $c=c_0$; $c_i=0$; $q_i=0$

B.C.1: at r=0; $\frac{\partial c_i}{\partial r}=0$ for t>0

B.C.2: at r=R; $\frac{\partial c_i}{\partial r}=\frac{R}{3\varepsilon_p D_e}\frac{\partial \overline{q}}{\partial t}$ for t>0.

The simulations of the mathematical model with all the equations (1 to 4) were performed using the programming language FORTRAN, with the software Compaq Visual Fortran Professional Edition 6.6. The numerical method of finite difference was used in this study to the solution of the three coupled nonlinear partial differential equations (2 to 4) of the model, following its initial and boundary conditions.

Eqs. (2) and (3) were discretized in space with 30 evenly spaced points along the column of adsorption, as long as Eq. (3) was discretized with 30 points along the pores of the adsorbent, between the center and the surface of the particle.

The DASSL subroutine was used for the solution of the equations, which was developed by Petzold in 1983-89 for the Lawrence Livermore National Laboratory, and won the first Wilkinson Prize for Numerical Software in 1991 [29]. All simulations were run on a Pentium Dual-Core (dual CPU) 2.16 GHz personal computer with 2 Gb of RAM.

The mathematical model was analyzed for its sensitivity and validated following the method of Wright and Glasser [22] to the experimental data of the two chitosanases. Experimental data were compared with simulation results to validate the modeling and simulation of breakthrough curves, examining the breakthrough times and assuming the starting points up to C/C_o=0.3. Quantitative evaluation of the fit between the curves was done by calculating the relative sum of the squares of the errors (RSSE) of the curves, as follows:

$$RSSE=\left[\sum_{i=1}^{m}\left(\frac{\left|e_i^2-(e_i^2-s_i^2)\right|}{e_i^2}\right)\right]\times\frac{100}{m}\% \quad (9)$$

where, e, and s, refer to experimental and simulated data points, respectively, m is the number of experimental points, and RSSE is a percentage where 100% represents perfect agreement between experimental and simulated curves. The parametric sensitivity analysis was done by increasing and decreasing each parameter by a factor of two and studied the effect on the breakthrough time, assuming the breakthrough value of C/C_o=0.15.

RESULTS AND DISCUSSION

1. Data Preparation

The determination of total protein with the Sedmak and Grossberg modified method [9] aimed to increase the accuracy of the data used in the mathematical model, once the ratio of absorbances, 595 nm/465 nm, was linear with protein concentration and improved the sensitivity of the purification assays.

In addition, all the purification experiments with expanded bed adsorption were performed without clarification (the cells were not removed). The process without clarification is a single step purification of the enzyme, which can be a great industrial advantage. From an economic point of view, the number of sequential operations required to achieve the desired degree of purity of a protein contributes significantly to the overall cost of the downstream process. It can represent up to 80% of the capital cost of the process due to the capital investment, amount of consumables needed for each step and the time required for each individual operation. In addition, the overall yield of purification is reduced with each step that is added to the process because of losses inherent to the product manipulation or even to production activity [3,9].

2. Estimation of Parameters

A chromatographic separation, such as expanded bed adsorption, is a complex purification process. It was developed through a series of measures that include a choice of high performance resins and techniques to select candidates suitable for a detailed investigation of retention behavior and capacity studies related to the variables that make up the process. These variables include, among others, particle size, pH, type and concentration of salt, solvents, additives, flow rate and temperature. Thus, the modeling, while avoiding the traditional trial and error, reduces the required number of experiments substantially, because the model parameters can be estimated from a very limited number of experiments [30].

In general, the parameters of a mathematical model concern the

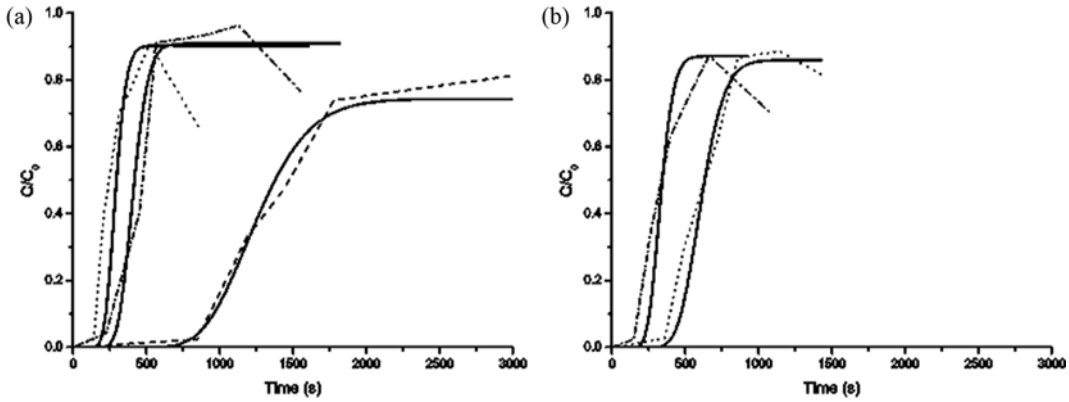

Fig. 2. (a) Breakthrough curves using Streamline DEAE adsorbent, where the solid lines are the mathematical model simulations with their experimental data, as follows: the dash-dotted line is Simulation 1; the dotted line is Simulation 2; and the dashed line is Simulation 3, respectively. (b) Breakthrough curves using Streamline SP XL, where the solid lines are the mathematical model simulations with their experimental data, as follows: the dash-dotted line is Simulation 4 and the dotted line is Simulation 5, respectively.

modeling of the purification of an enzyme broth, clarified, containing a single enzyme model [4,23]. In the present study, however, we used a crude enzyme broth, i.e., broth not clarified. In addition, all model parameters are global because they represent the purification of two *Metarhizium anisopliae* chitosanases. The initial values of the global parameters were obtained from literature [22,23, 31,32] or calculated [33], and then were adjusted by a specific and iterative routine of gradual reduction of residues, obtaining the final values shown in Table 1.

3. Model Validation

The mathematical model was validated with simulations performed with the adjusted parameters (Table 1), and using the experimental data obtained according to Fig. 1 and previous description. The comparative results are shown in Fig. 2(a) and (b) for the Streamline DEAE and SP XL adsorbents, respectively.

Fig. 2(a) and (b) shows visually a high degree of fit between experimental and simulated points, which was confirmed by calculating the relative sum of the squares of the errors (RSSE) for the curves, as shown in Table 2.

The RSSE values showed an average of 95.21% and 93.88% for Streamline DEAE and SP XL adsorbents, respectively, with a global average of 94.68%, resulting in a very good fit. Note that instead of pure protein (as in most published studies), we used a non-clarified fermentation broth (cell), and therefore these results are for the two extracellular chitosanases from *Metarhizium anisopliae* fungus.

Table 2. Relative sum of the squares of the errors (RSSE) from the five different simulations with the mathematical model of the purification of two chitosanases from *Metarhizium anisopliae* with expanded bed adsorption

Simulation	Adsorbent	Superficial velocity ($m \cdot s^{-1}$)	RSSE (%)
1	DEAE	4.17×10^{-4}	97.95
2	DEAE	7.22×10^{-4}	92.36
3	DEAE	1.11×10^{-4}	95.31
4	SP XL	5.69×10^{-4}	91.49
5	SP XL	2.64×10^{-4}	96.26
		Average	94.68

4. Parametric Sensitivity Analysis

Many key parameters of an expanded bed adsorption process

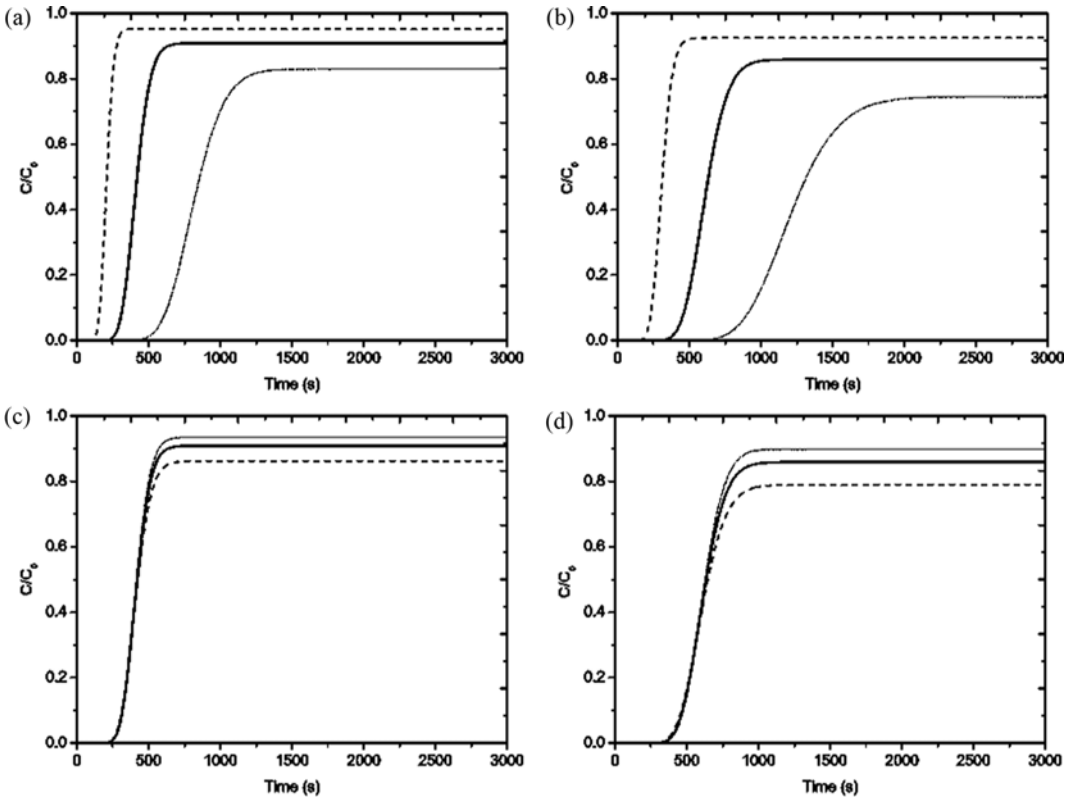

Fig. 3. (a) Breakthrough curves with sensitivity results for superficial velocity (u) variation, with Streamline DEAE adsorbent, where the solid curve is the reference (Simulation 1). The dashed line and the dash-dotted line are simulations with the 2u (8.34×10^{-4} $m \cdot s^{-1}$) and u/2 (2.08×10^{-4} $m \cdot s^{-1}$) of this reference (4.17×10^{-4} $m \cdot s^{-1}$), respectively. (b) Streamline SP XL adsorbent, where the solid curve is the reference (Simulation 5). The dashed line and the dash-dotted line are simulations with the 2u (5.28×10^{-4} $m \cdot s^{-1}$) and u/2 (1.32×10^{-4} $m \cdot s^{-1}$) of this reference (2.64×10^{-4} $m \cdot s^{-1}$), respectively. (c) Breakthrough curves with sensitivity results for variation of axial dispersion coefficient (D_{ax}), with Streamline DEAE adsorbent, where the solid curve is the reference (Simulation 1). The dashed line and the dash-dotted line are simulations with the $2D_{ax}$ (3.0×10^{-7} $m^2 \cdot s^{-1}$) and the $D_{ax}/2$ (0.75×10^{-7} $m^2 \cdot s^{-1}$) of this reference (1.5×10^{-7} $m^2 \cdot s^{-1}$), respectively. (d) Streamline SP XL adsorbent, where the solid curve is the reference (Simulation 5). The dashed line and the dash-dotted line are simulations with the $2D_{ax}$ (3.0×10^{-7} $m^2 \cdot s^{-1}$) and $D_{ax}/2$ (0.75×10^{-7} $m^2 \cdot s^{-1}$) of this reference (1.5×10^{-7} $m^2 \cdot s^{-1}$), respectively.

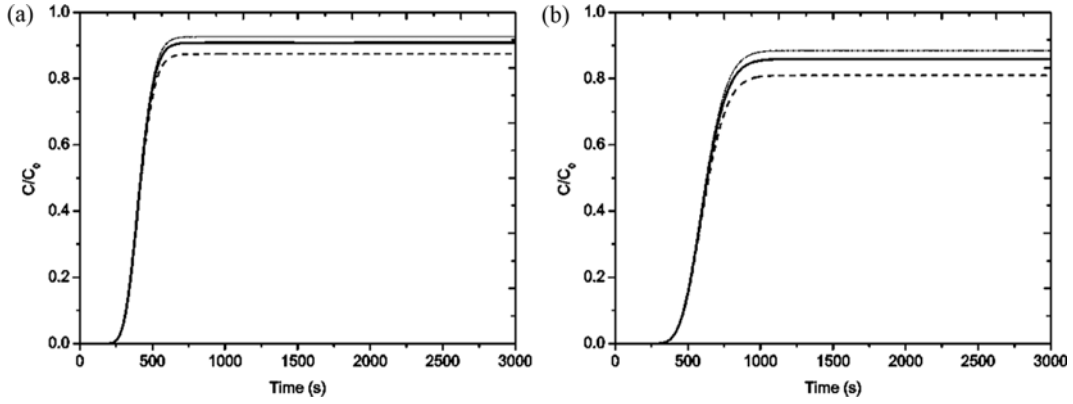

Fig. 4. (a) Breakthrough curves with sensitivity results for variation of film mass-transfer coefficient (k_f), with Streamline DEAE adsorbent, where the solid curve is the reference (Simulation 1). The dashed line and the dash-dotted line are simulations with the $2k_f$ (1.2×10^{-8} m·s^{-1}) and $k_f/2$ (0.3×10^{-8} m·s^{-1}) of this reference (0.6×10^{-8} m·s^{-1}), respectively. (b) Streamline SP XL adsorbent, where the solid curve is the reference (Simulation 5). The dashed line and the dash-dotted line are simulations with the $2k_f$ (1.2×10^{-8} m·s^{-1}) and $k_f/2$ (0.3×10^{-8} m·s^{-1}) of this reference (0.6×10^{-8} m·s^{-1}), respectively.

are connected and a parametric sensitivity analysis is a way to uncouple and study the contribution of each parameter on breakthrough behavior, since many of these key parameters cannot be uncoupled in an experimental setup. We used the methodology of Wright and Glasser [22], in which each parameter was increased and decreased by a factor of 2 to study the effect on the breakthrough time for C/C_0=0.15. Thus, three key parameters were investigated, as suggested in the literature [22,23,34]: the hydrodynamic parameters superficial velocity and axial dispersion coefficient, and the mass transfer parameter film mass-transfer coefficient, which is also related to the hydrodynamic parameters.

The change in superficial velocity is known to significantly alter the other operating conditions of a chromatographic separation, such as expanded bed adsorption [35]. The axial dispersion and the film mass-transfer coefficients are distinct sources of non-equilibrium effect to the adsorption-desorption kinetics. The first one is the axial dispersion in the interstitial volume, which combines longitudinal diffusion and eddy dispersion in the moving eluent. The second one is the mass transfer resistance across the external surface area of the stationary phase [36].

The use of factor 2 in the sensitivity analysis showed that the model is very sensitive to changes in the values of superficial velocity (Fig. 3(a) and (b)), but relatively insensitive to variations in axial dispersion coefficient (Fig. 3(c) and (c)) and film mass-transfer coefficient, as showed in Fig. 4(a) and (b).

When the superficial velocity was doubled, the breakthrough time for C/C_0=0.15 was reduced by half, and when the superficial velocity was reduced by half, the breakthrough time doubled, as shown in Fig. 4(a) and (b) and in Table 3. Such effects can be explained by the increase in residence time when the superficial velocity was reduced, providing more time for adsorption and, consequently, increasing the breakthrough time. The opposite happened when the superficial velocity was increased. The breakthrough time variation of the axial dispersion coefficient, using the same factor 2 and

Table 3. Results from parametric stimulation of the model, with Streamline DEAE and Streamline SP XL

Parameter	Stimulus	C/Co	Reference (s)	Breakthrough time with stimulus (s)	Variation (%)
Streamline DEAE					
Superficial linear velocity (u)	2u	0.15	330.48	168.06	−49.15
	u/2	0.15	330.48	669.10	102.47
Axial dispersion coefficient (D_{ax})	$2D_{ax}$	0.15	330.48	331.80	0.40
	$D_{ax}/2$	0.15	330.48	336.00	1.67
Film mass-transfer coefficient (k_f)	$2k_f$	0.15	330.48	336.00	1.67
	$k_f/2$	0.15	330.48	333.60	0.95
Superficial velocity of 4.17×10^{-4} m·s^{-1} (reference: Simulation 1)					
Streamline SP XL					
Superficial linear velocity (u)	2u	0.15	497.40	249.60	−49.82
	u/2	0.15	497.40	991.20	99.28
Axial dispersion coefficient (D_{ax})	$2D_{ax}$	0.15	497.40	491.40	−1.21
	$D_{ax}/2$	0.15	497.40	500.40	0.60
Film mass-transfer coefficient (k_f)	$2k_f$	0.15	497.40	500.49	0.62
	$k_f/2$	0.15	497.40	495.60	−0.36
Superficial velocity of 2.64×10^{-4} m·s^{-1} (reference: Simulation 5)					

with C/C_0=0.15, was negligible (<2%), i.e., smaller than the effect of the variation of superficial velocity, as shown in Fig. 3(c) and (d). The variation of the film of mass-transfer coefficient had the same negligible effect on the breakthrough time, as shown Fig. 4(a) and (b) and also in Table 3. All these effects of variation of the three key parameters are consistent with the literature [22,35,37].

Therefore, the two ion-exchanger and widely used adsorbents, Streamline DEAE and Streamline SP XL, had similar performance in relation to hydrodynamics and mass transfer. They confirmed an expectation regarding the similarity of the physicochemical characteristics that they have (density, diameter, covered with agarose, macropores size and size distribution of particles, among others).

Thus, the results show that the model is suitable for the experimental data during purification of chitosanases with expanded bed adsorption and feeding the adsorption column with crude enzyme broth (without clarification). In this study, the breakthrough curve of enzyme activity had a quite similar profile of total protein (data not shown); therefore, it was modeled like a pure standard protein, such as bovine serum albumin or lysozyme, for example [22,27].

CONCLUSIONS

The model was validated for the Streamline DEAE and Streamline SP XL adsorbents, anion and cation exchange resins, respectively. These two adsorbents had similar performance in relation to hydrodynamics and mass transfer, with an average high degree of fit between simulated and experimental data (94.68%), and the results of the parametric sensitivity analysis agree with the literature. Thus, all the results of the present study show that the mathematical model is suitable for the purification of the two chitosanases from *Metarhizium anisopliae*, with expanded bed adsorption and without clarification, aiming at the reduction of unit operations in future projects of separation processes, thereby reducing capital and operating costs.

NOMENCLATURE

c : concentration in particle pore [kg/m^3]
c_0 : initial bulk-phase protein concentration in particle pore [kg/m^3]
c_i : protein concentration in particle pore [kg/m^3]
C : bulk-phase concentration of enzyme [kg/m^3]
C_o : feedstock concentration of enzyme [kg/m^3]
C_f : local equilibrium concentration at particle surface [kg/m^3]
C^* : protein concentration in the liquid at equilibrium [kg/m^3]
D_e : effective solid-phase diffusion coefficient [m^2/s]
D_{ax} : axial dispersion coefficient [m^2/s]
D_s : solid dispersion coefficient [m^2/s]
e : experimental data points
H : expanded-bed height [m]
H_o : settled-bed height [m]
k_f : film mass-transfer coefficient [m/s]
k_d : equilibrium dissociation constant [kg/m^3]
m : number of experimental points
q : adsorbed concentration of protein [kg/m^3]
q^* : concentration of the adsorbed protein on the resin [kg/m^3]
$\bar{q}$: averaged adsorbent phase concentration [kg/m^3]
q_i : protein concentration adsorbed on the particle [kg/m^3]
q_{max} : maximum adsorbed concentration of enzyme [kg/m^3]
r : radial position in the particle [m]
R : particle radius [m]
RSSE : relative sum of the squares of the errors
s : simulated data points
t : time [s]
u : superficial linear velocity [m/s]
z : axial position in the column [m]

Greek Letters

ε : liquid void fraction in the expanded-bed
ε_o : liquid void fraction in the packed-bed
ε_p : adsorbent effective porosity
ρ_L : solution density [kg/m^3]
ρ_p : adsorbent density [kg/m^3]

ACKNOWLEDGEMENTS

The authors thank the National Council for Scientific and Technological Development (CNPq) and Coordination of Improvement of Higher Education (CAPES) for financial support.

REFERENCES

1. J. M. Mollerup, T. B. Hansen, S. Kidal and A. Staby, *J. Chromatogr. A*, **1177**(2), 200 (2008).
2. W. B. Yap, B. T. Tey, N. B. M. Alitheen and W. S. Tan, *J. Chromatogr. A*, **1217**, 3473 (2010).
3. J. Zhao, S. Yao and D. Lin, *Chinese J. Chem. Eng.*, **17**(4), 678 (2009).
4. C. C. Moraes, M. A. Mazutti, M. I. Rodrigues, F. M. Filho and S. J. Kalil, *J. Chromatogr. A*, **1216**, 4395 (2009).
5. E. E. G. Rojas, J. S. Reis Coimbra, L. A. Minim, S. R. H. Saraiva and C. S. A. S. Silva, *J. Chromatogr. B*, **840**(2), 85 (2006).
6. G. S. Padilha, J. C. Curvelo-Santana, R. M. Alegre and E. B. Tambourgi, *J. Chromatogr. B*, **877**(5-6), 521 (2009).
7. L. M. Pinotti, L. P. Fonseca, D. M. F. Prazeres, D. S. Rodrigues, E. R. Nucci and R. L. C. Giordano, *Biochem. Eng. J.*, **44**, 111 (2009).
8. C. Hidayat, M. Takagi and T. Yoshida, *J. Biosci. Bioeng.*, **97**, 284 (2004).
9. E. S. Santos, R. Guirardello and T. T. Franco, *J. Chromatogr. A*, **944**(1-2), 217 (2002).
10. X. Chen, W. Xia and X. Yu, *Food Res. Internat.*, **38**, 315 (2005).
11. L. Santi, W. O. Beys da Silva, M. Berger, J. A. Guimarães, A. Schrank and M. H. Vainstein, *Toxicon*, **55**, 874 (2010).
12. C. F. Assis, N. Araújo, M. Pagnoncelli, M. S. Pedrini, G. R. Macedo and E. S. Santos, *Bioproc. Biosys. Eng.*, **33**(7), 893 (2010).
13. J. Wang, W. Zhou, H. Yuan and Y. Wang, *Carbohyd. Res.*, **343**, 2583 (2008).
14. W. Xia, P. Liu, J. Zhang and J. Chen, *Food Hydrocol.*, **25**, 170 (2011).
15. K. T. Shen, M. H. Chen, H. Y. Chan, J. H. Jeng and Y. J. Wang, *Food Chem. Toxicol.*, **47**, 1864 (2009).
16. M. Artan, F. Karadeniz, M. Z. Karagozlu, M. M. Kim and S. K. Kim, *Carbohyd. Res.*, **345**, 656 (2010).
17. M. Senevirathne, C. B. Ahn and J. Y. Je, *Carbohyd. Polym.*, **83**(2), 995 (2011).
18. D. H. Ngo, Z. J. Qian, T. S. Vo, B. Ryu, D. N. Ngo and S. K. Kim,

Carbohyd. Polym., **88**(2), 743 (2012).
19. L. T. Fan, Y. C. Yang and C. Y. Wen, *AIChE J.*, **6**(3), 482 (1960).
20. S. Veeraraghavan, L. T. Fan and A. P. Mathews, *Chem. Eng. Sci.*, **44**(10), 2333 (1989).
21. T. V. Thelen and W. Fred Ramirez, *Chem. Eng. Sci.*, **52**(19, 3333 (1997).
22. P. R. Wright and B. J. Glasser, *AIChE J.*, **47**, 474 (2001).
23. P. Li, G. Xiu and A. E. Rodrigues, *AIChE J.*, **51**(11), 2965 (2005).
24. M. M. H. El-Sayed and H. A. Chase, *Biochem. Eng. J.*, **49**, 221 (2010).
25. L. J. Bruce, R. H. Clemmitt, D. C. Nash and H. A. Chase, *J. Chem. Technol. Biotechnol.*, **74**(3), 264 (1999).
26. P. Gardner, N. Willoughby, R. Hjorth, K. Lacki and N. Titchener-Hooker, *Biotechnol. Bioeng.*, **87**(3), 347 (2004).
27. X. D. Tong, B. Xue and Y. Sun, *Biochem. Eng. J.*, **16**, 365 (2003).
28. O. Levenspiel, *Chemical reaction engineering*, Wiley, New York (1999).
29. S. Li, L. Petzold and W. Zhu, *Appl. Num. Mathemat.*, **32**, 161 (2000).
30. J. M. Mollerup, T. B. Hansen, S. Kidal, L. Sejergaard and A. Staby, *Fluid Phase Equilib.*, **261**, 133 (2007).
31. J. Yun, D. Q. Lin and S. J. Yao, *J. Chromatogr. A*, **1095**, 16 (2005).
32. L. S. Conrado, V. Veredas, E. S. Nóbrega and C. C. Santana, *Braz. J. Chem. Eng.*, **22**(4), 501 (2005).
33. D. Kunii and O. Levenspiel, *Fluidization engineering*, Robert E. Krieger Publishing Company, New York (1977).
34. D. Nagrath, F. Xia and S. M. Cramer, *J. Chromatogr. A*, **1218**, 1219 (2011).
35. Y. K. Chang and H. A. Chase, *Biotechnol. Bioeng.*, **49**(5), 512 (1996).
36. F. Gritti and G. Guiochon, *J. Chromatogr. A*, **1218**(22), 3476 (2011).
37. A. Karau, C. Benken, J. Thömmes and M. R. Kula, *Biotechnol. Bioeng.*, **55**(1), 54 (1997).